Supplementary Information

A new method for detailed discharge and volume measurements of debris flows based on high-frequency 3D LiDAR point clouds; Illgraben, Switzerland

Raffaele Spielmann[a,b] and **Jordan Aaron**[a,b]

raffaele.spielmann@erdw.ethz.ch
jordan.aaron@erdw.ethz.ch

[a] Chair of Engineering Geology, Geological Institute, Department of Earth Sciences, ETH Zürich, Sonneggstrasse 5, 8092 Zurich, Switzerland

[b] Swiss Federal Institute for Forest, Snow and Landscape Research WSL, Zürcherstrasse 111, 8903 Birmensdorf, Switzerland

Corresponding author:
Raffaele Spielmann (raffaele.spielmann@erdw.ethz.ch)
ETH Zürich, Sonneggstrasse 5, 8092 Zurich, Switzerland

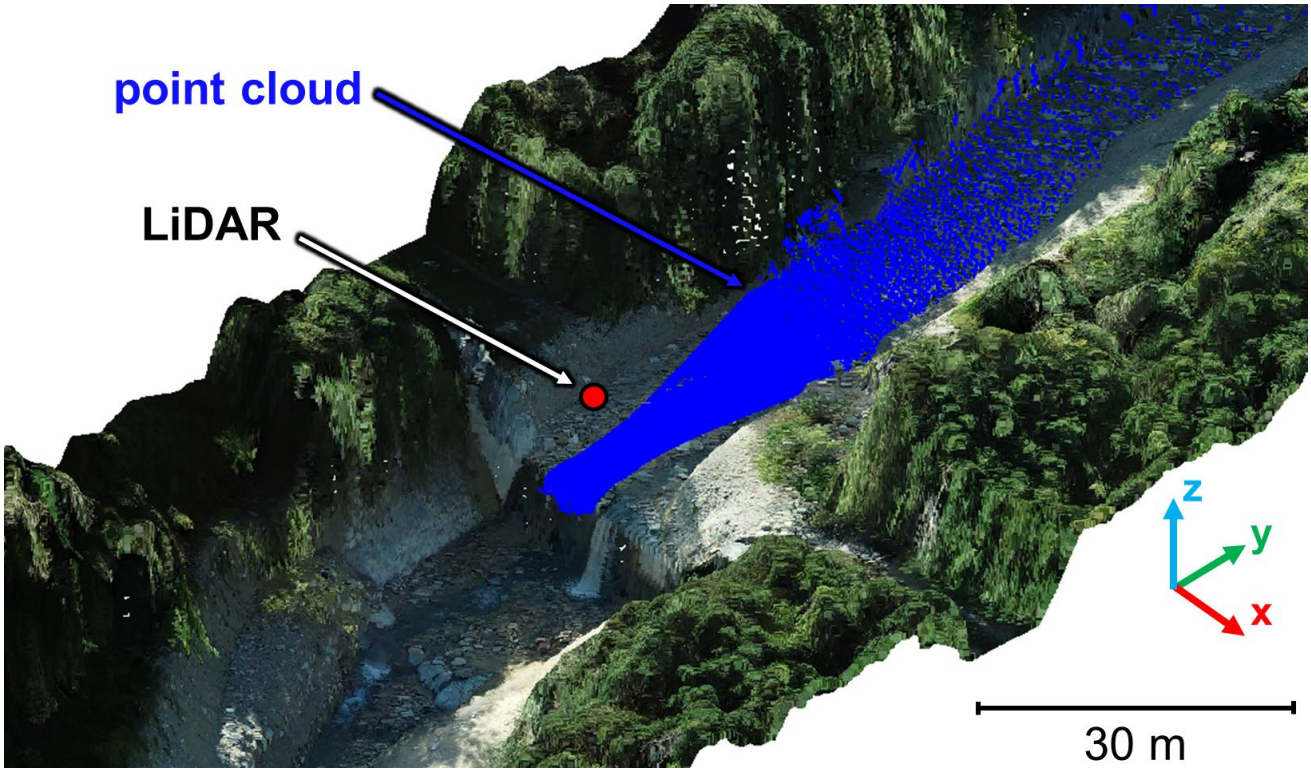

Figure SI 1: Example of a point cloud recorded by the LiDAR sensor (blue dots) at the monitoring station “Gazoduc” on top of a point cloud from a photogrammetric drone flight (de Haas et al., 2022). The arrows indicate the direction of the axes of the *bed-parallel coordinate system* used in the present work (*x*-axis parallel to the crest of the check dam, *y*-axis parallel and *z*-axis perpendicular to the channel bed, respectively; visualization in *CloudCompare*).

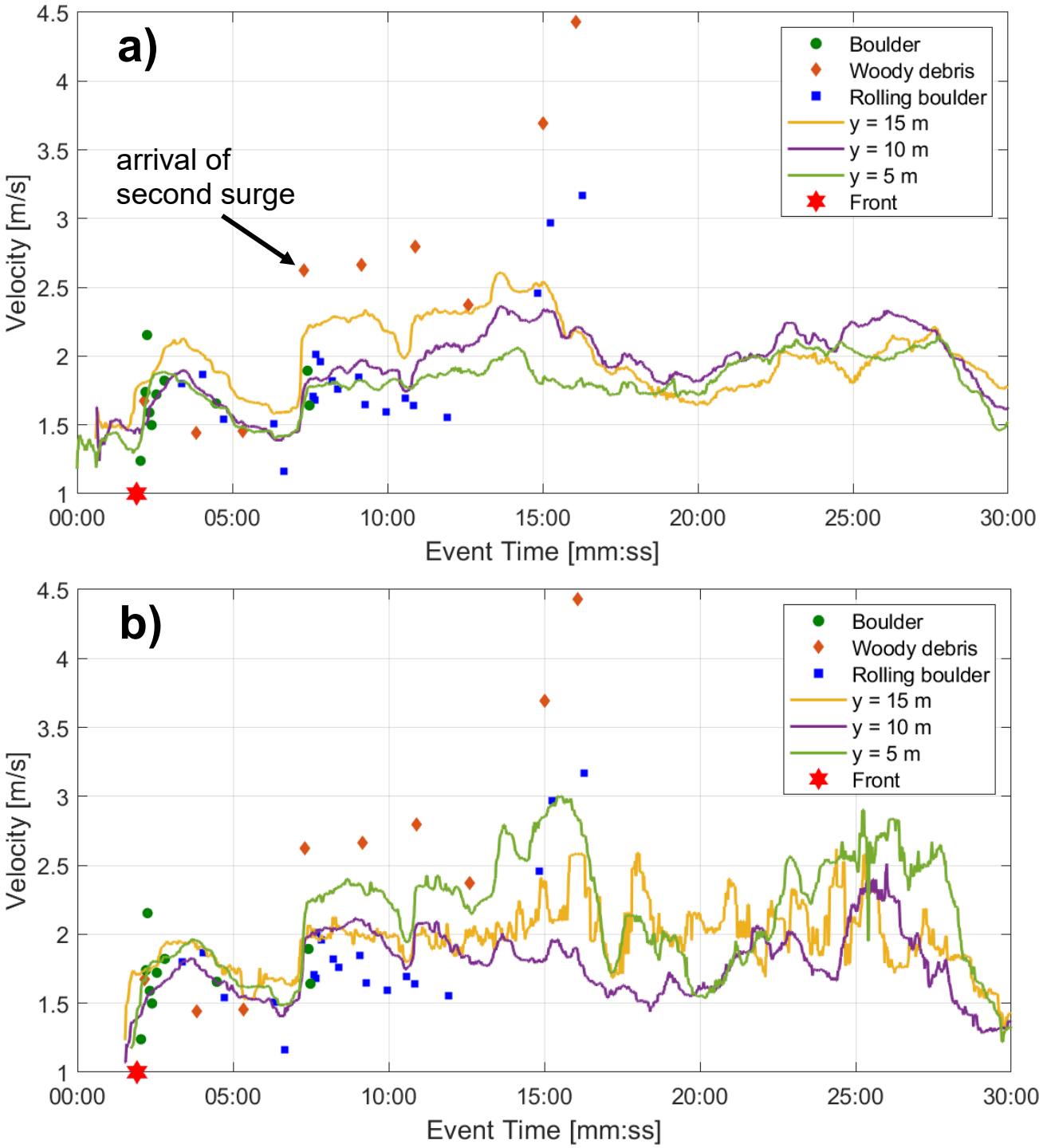

Figure SI 2: Comparison of objects (large rolling boulders, boulders, woody debris; cf. Spielmann, 2022) manually identified and tracked in the LiDAR point clouds and automatically derived surface velocities based on the a) camera1-ortho method as well as the b) hillshade method (see main text and Aaron et al., 2023). The manual velocities are mean velocities for a given object over the entire duration that it was tracked, i.e. over the entire channel segment upstream of the sensor (see Figure SI 1). The automated velocities represent average velocities across the channel at a given channel section (upstream of sensor distance *y* in meters; see Figure 5 in the main text). A piece of woody debris in a) corresponds to the arrival of the second surge and was used to estimate the velocity of this second surge (~ 2.5 m/s, see Table SI 1). The red star indicates the (mean) velocity of the flow front (see also Figure 8 in the main text).

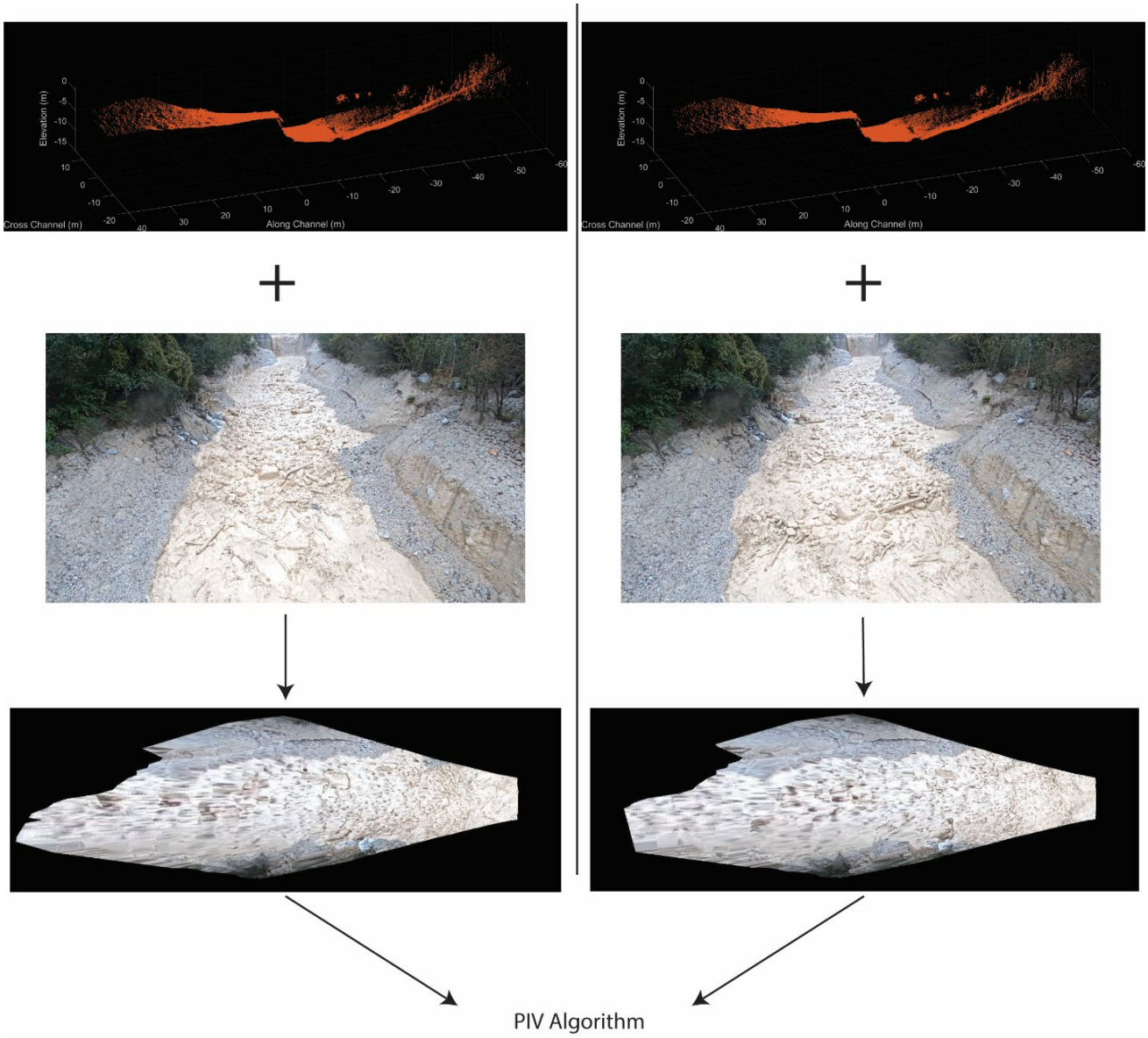

Figure SI 3: Description of the process to generate orthophotos by fusing the LiDAR point clouds and camera data. Camera images are orthorectified using the point cloud data, and subsequently input into a PIV algorithm to generate a dense 2D velocity field. The 2D orthophoto displacements are then re-projected onto the corresponding point clouds to derive the z-component of the velocity (see main text and Aaron et al., 2023, for details).

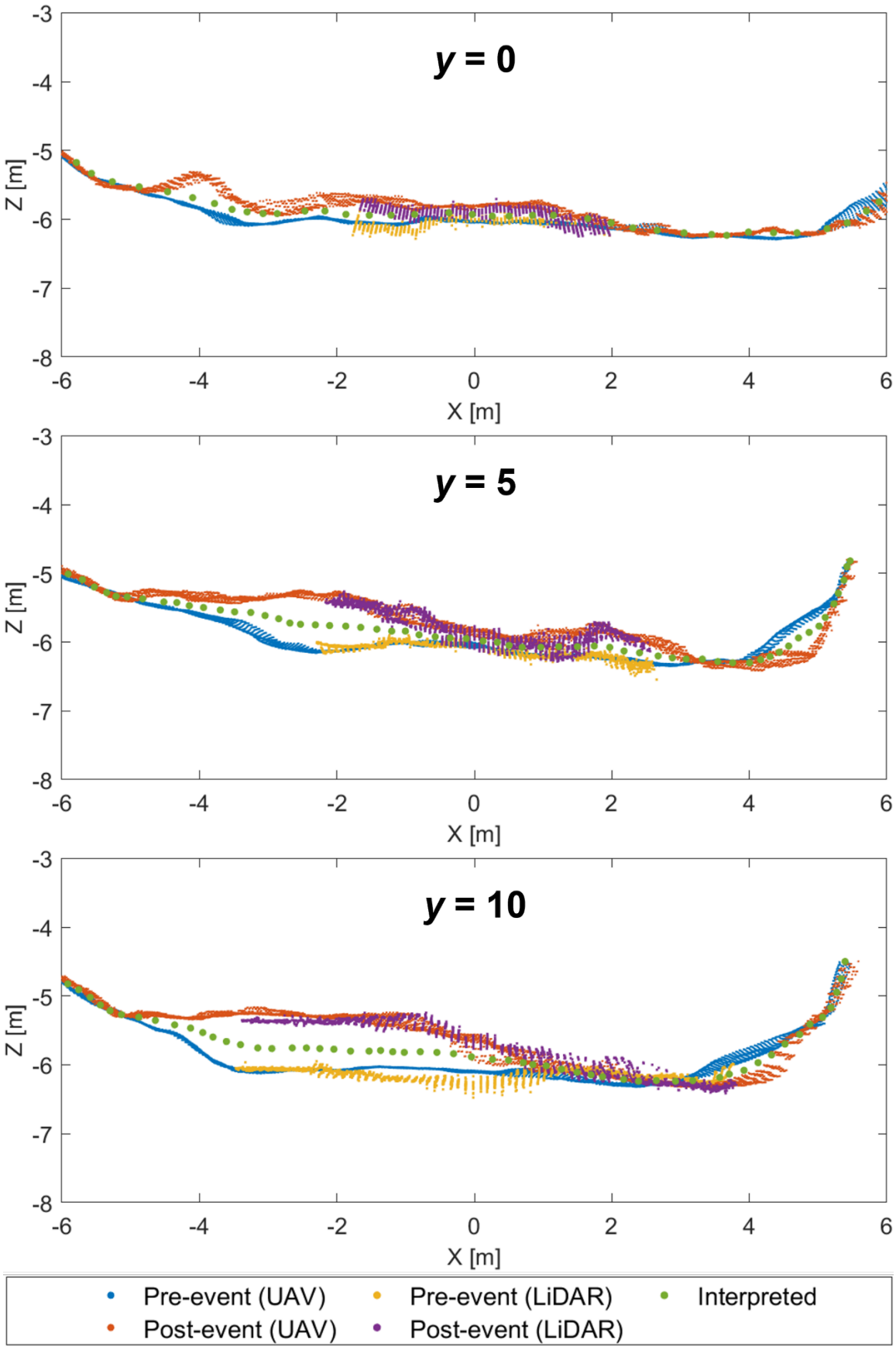

Figure SI 4: Channel geometry scenarios (pre-event, post-event and intermediate) for the channel sections $y = 0$ m, $y = 5$ m and $y = 10$ m upstream of the sensor. The points from the point clouds represent all points within a 1 m wide slice at each of these channel sections, before they were interpolated according to the description in Section 3.4. As the LiDAR sensor does not cover the full channel width in these sections, we used the UAV-based channel geometries to measure the cross-sectional area.

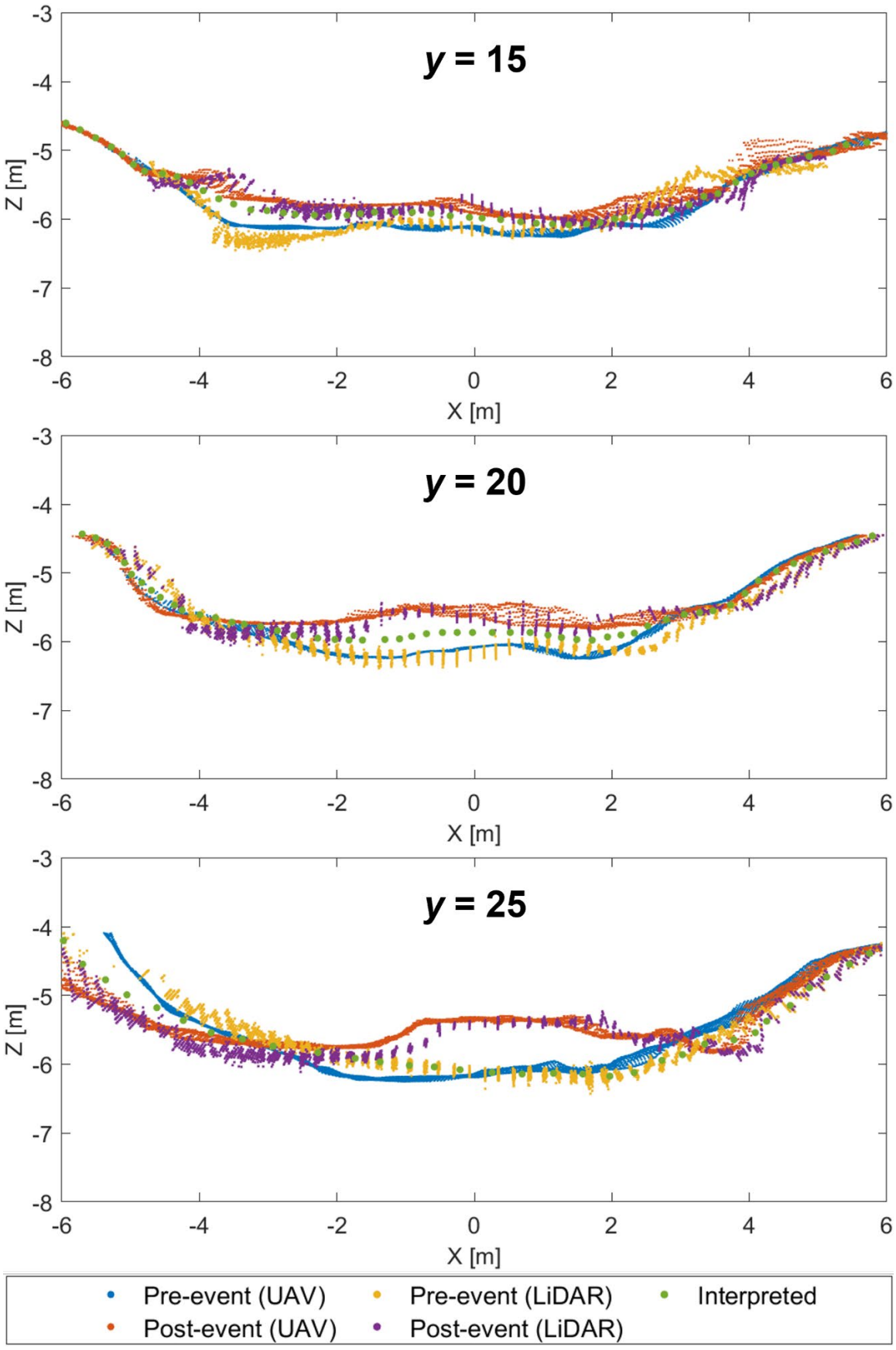

Figure SI 5: Channel geometry scenarios (pre-event, post-event and intermediate) for the channel sections y = 15 m, y = 20 m and y = 25 m upstream of the sensor. As the LiDAR sensor does not cover the full channel width in the section y = 15 m, we used the UAV-based channel geometries to measure the cross-sectional area. However, in sections y = 20 m and y = 25 m, we used the LiDAR-based channel geometries.

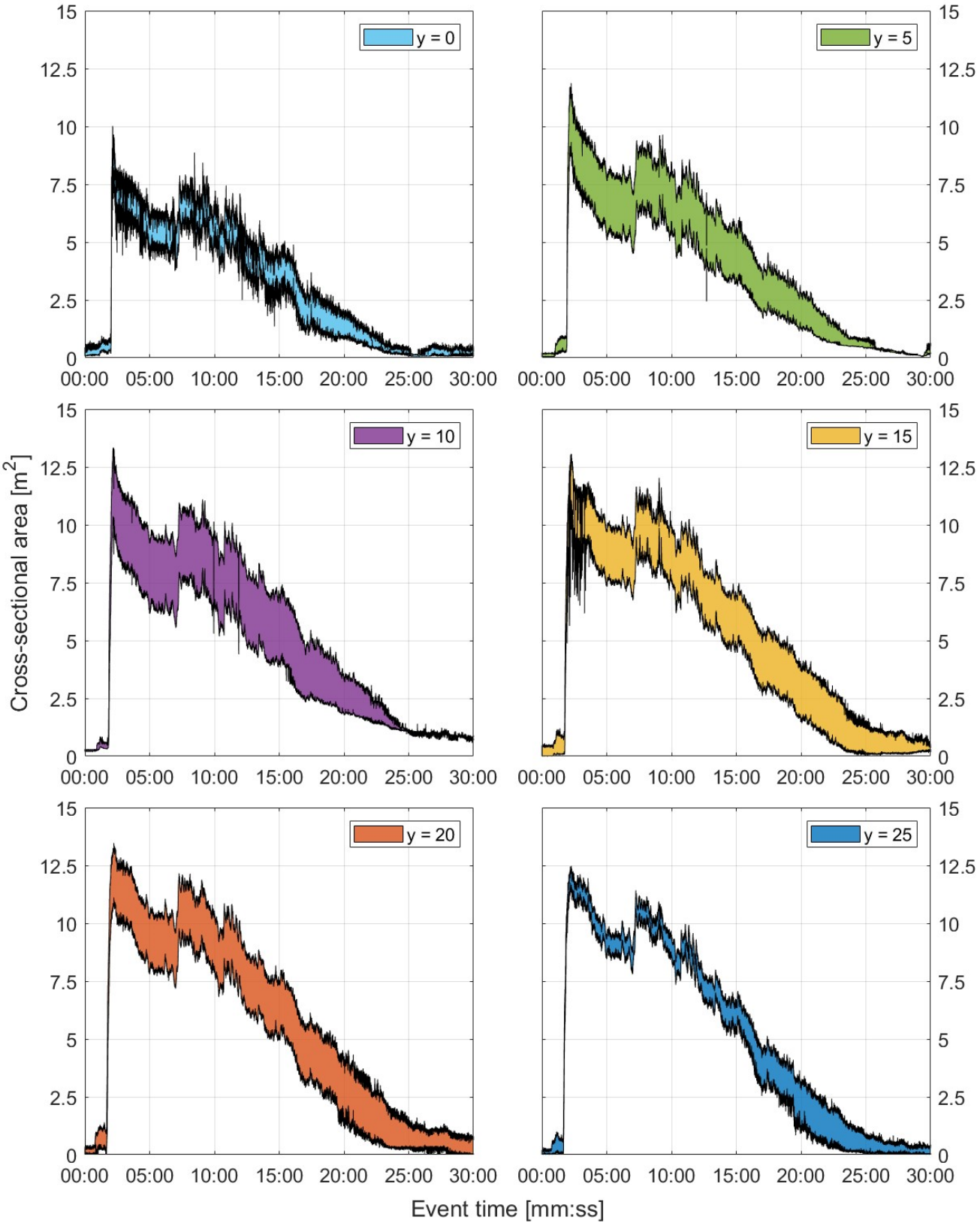

Figure SI 6: Cross-sectional area for each channel section (upstream of sensor distance y in meters) automatically derived from the point-cloud data (at a frequency of 10 Hz). The colored area represents the range of the cross-sectional area based on the selected basal geometry scenario (upper line: pre-event geometry, lower line: post-event geometry). Please note that the bed geometry for the more downstream sections (y = 0 m, y = 5 m, y = 10 m, y = 15 m) is based on data from photogrammetric drone (UAV) flights and that the flow surface had to be extrapolated towards the channel banks in these sections, whereas the more upstream sections (y = 20 m and y = 25 m) rely on LiDAR data only. An overview of these channel sections is shown in Figure 5 in the main text.

Table SI 1: Velocities (u) used to derive the discharge based on the event and surge scale methodologies (e.g. Lapillonne et al., 2023), either over the full scale of the debris-flow event (event scale) or by considering individual surges (surge scale), according to Equation 2 (main text).

	Front Arrival / First Surge (before 07:20)	**Second Surge** (after "velocity jump") (after 07:20)
Event Scale Method	1.0 m/s	1.0 m/s
Surge Scale Method	1.0 m/s	2.5 m/s

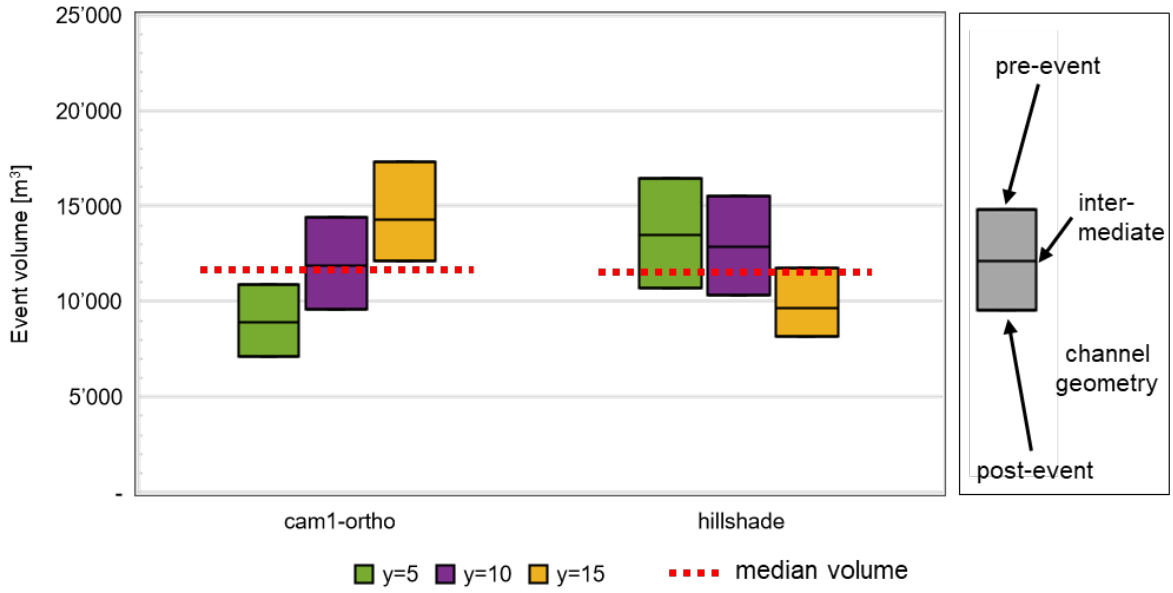

Figure SI 7: Event volumes for the 19 Sept. 2021 debris flow, based on velocity datasets with different filtering parameters than in Figure 12 (i.e. $-0.2\ \mathrm{m/s} \leq v_x \leq 0.2\ \mathrm{m/s}$ and $-4\ \mathrm{m/s} \leq v_y \leq -0.2\ \mathrm{m/s}$ for the velocity components along the x- and y-axes, respectively) and velocity factors (VF = 1.0 for both datasets; cf. Figure 11 and Figure 12 in main text). This calculation was performed as part of a sensitivity analysis of the velocity data. The resulting median volumes are 11 900 m^3 for camera1-ortho and 11 730 m^3 for the hillshade method (cf. also Figure 12).